

# A Novel Feedback Linearisation Control of Flyback Converter

Research paper

Miklos Csizmadia\*<sup>ORCID</sup>, Miklos Kuczmann<sup>ORCID</sup>

Széchenyi István University, Győr, Hungary

Received: 16, November 2022; Accepted: 04, January 2023

**Abstract:** This paper presents a novel approach for feedback linearisation in a continuous conduction mode (CCM) of the flyback converter. Due to the unstable zero dynamics, a flyback converter has highly non-linear behaviour. Flyback converters mostly use the indirect (current) control mechanism. In contrast, this paper shows a direct control of the output voltage of a flyback converter with feedback linearisation (a non-linear control method). In the designed controller, an error integrator is applied to improve the dynamic and steady-state behaviour of the controller. To design the feedback linearisation method, the state-space averaged model is determined. The converter and the proposed control are tested in a MatLab/Simulink environment, and the results are compared with other optimal controller methods. The results provide feedback about the efficiency and practical implementation of the proposed method.

**Keywords:** CCM flyback converter • isolated converter • feedback linearisation • non-minimum phase • power electronics

## 1. Introduction

Currently, the improvement of the power electronic equipment has led to momentous growth in many industrial segments, such as e-mobility or renewable energy (Pesce et al., 2021; Ramos-Paja et al., 2021; Tseng and Fan, 2021). A common feature of the above industrial segments is that the auxiliary circuits of the equipment require a stable direct current (DC) voltage, which is achieved by a DC/DC or alternating current (AC)/DC converter. Requirements for the auxiliary power supply include high power density, easy voltage step-up or step-down, galvanic isolation and simple construction/low number of components. Considering the switched-mode power supply (SMPS) topologies currently used in power electronic systems, the flyback converter satisfies the above conditions: it is well-suited for low-to-medium power range applications up to several hundred watts and can be applied in both AC/DC and DC/DC conversions with galvanic isolation (Khairy et al., 2015; Mohanty et al., 2015; Paul and Bhuvanesh, 2015; Szeli et al., 2013). On the other hand, flyback converters also power many everyday electrical appliances such as digital versatile disc (DVD) players, mobile phones and laptop chargers (Yin et al., 2020).

The flyback converter – like most switching converters – exhibits non-linear behaviour, which makes the controller design more complex. For this reason, a non-linear controller is needed to achieve good dynamic and steady-state behaviour. A further important requirement for such circuits is robust behaviour, that is, being insensitive to changes in input voltage, parameter or load. For many control circuits, the presence of a steady-state fault is an additional problem. In the literature, many advanced non-linear and optimal control strategies, such as linear quadratic controller, sliding mode controller (SMC), H-infinity, or feedback linearisation, have been published to achieve a good closed-loop performance of the flyback converter (Bouziiane et al., 2015; Mandal and Mishra, 2018; Prasad and Kumar, 2018). Taking into account our previous results, feedback linearisation has been applied to non-isolated converters with good results: the method has been transformed into a framework and the modifications

\* Email: csizmadia.miklos@sze.hu

have improved the dynamic behaviour and minimised the steady-state error. Accordingly, this paper presents a novel form of control framework based on feedback linearisation via the flyback converter.

The structure of the paper is as follows. Section 2 describes the operation of the flyback converter with the circuit diagram and the important equations and diagrams, and Section 3 summarises the state-space equations of the continuous conduction mode (CCM) operation. The remaining sections deal with the design of the feedback linearisation-based controller (Sections 4 and 5) and present the simulation results (Section 6).

## 2. Operation Principle of Flyback Converter

The circuit diagram of the flyback converter is shown in Figure 1. The circuit includes the high-frequency transformer, the switching element (which is more often a metal–oxide–semiconductor field-effect transistor [MOSFET]), the output diode (D), and the capacitor (C). It is evident that the output (load) voltage is equal to the capacitor voltage. An important part of this figure is the magnetising inductance, which is transformed to the primary side of the transformer. It can be obtained from the following equation:

$$L_p = L_l + L_m \quad (1)$$

where  $L_p$  is the primer inductance,  $L_l$  is the leakage inductance and  $L_m$  is the magnetising inductance of the transformer. The primer and the leakage inductances of the transformer are measurable parameters.

The operation of the flyback converter can be separated into two modes, depending on the inductor current in each cycle. If the switching element (SW) turns on before the primer inductor is completely discharged, then the current in the inductor never reaches zero. This operation is called also CCM. However, the off time  $t_{off}$  lasts long enough for the primary inductor to fully discharge, so there is a time interval during which the current in the inductor reaches zero. This causes both the output diode D and the switching element (SW) to be in an off-state and is called discontinuous conduction mode (DCM) (Iqbal and Abbas, 2014).

The DCM operation is used typically in a low-power application for the following reasons: (i) the switching semiconductor element has a lower power loss and lower stress; (ii) DCM reduces the rectifier losses and usually reduces the transformer size requirement as well. At the same time, the DCM operation has higher peak currents, which also affects the selection/design of the transformer and the switching element. CCM operation is commonly used for medium- or high-power applications. The CCM operation has been investigated in detail in a previous article (Mohammed and Nafie, 2015).

In the CCM region, two different intervals can be defined depending on the state of the switching element (SW) (Iqbal and Abbas, 2014): during on-time, there is no energy transfer to the secondary side due to the reverse bias of the secondary side diode (D). The output is supplied with the secondary side capacitor (C). If the switching element

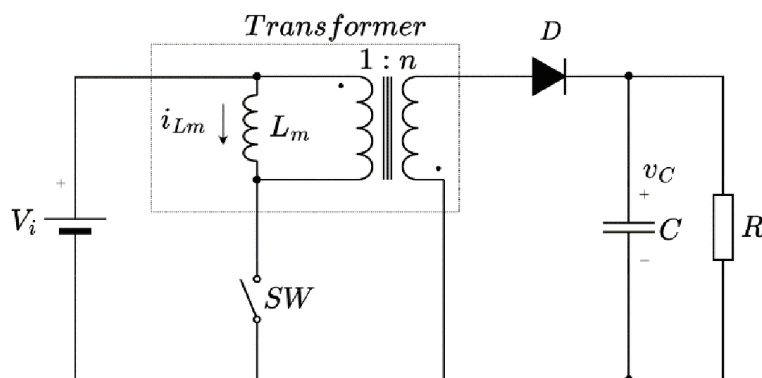


**Fig. 1.** Circuit diagram of the flyback converter. R, L, C and N symbolise the output load, inductance, capacitance and turn ratio, respectively, of the converter.  $L_m$ , magnetising inductance; SW, switching element.

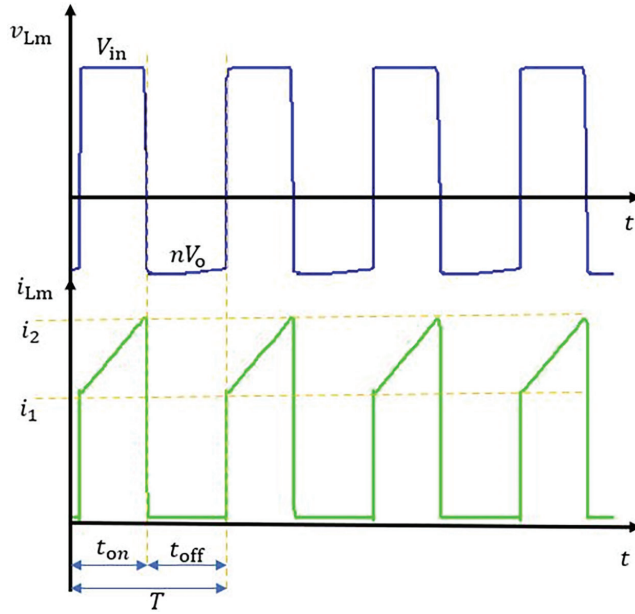


**Fig. 2.** Waveforms of the magnetising inductance of flyback converter in CCM (LTspice software). CCM, continuous conduction mode;  $L_m$ , magnetising inductance.

(SW) goes off-state, the stored energy in a leakage inductance is transferred to the load (R). The waveforms of the magnetising inductance's voltage and current are shown in Figure 2.

The system equations of the flyback converter are the following (Iqbal and Abbas, 2014): when the switching element (SW) is on ( $0 < t < dT_s$ ):

$$\begin{aligned} \frac{di_{Lm}}{dt} &= \frac{V_i}{L_m}, \\ \frac{dv_C}{dt} &= -\frac{v_C}{RC}. \end{aligned} \quad (2)$$

When the switching element (SW) is off ( $dT_s < t < T_s$ ):

$$\begin{aligned} \frac{di_{Lm}}{dt} &= \frac{Nv_C}{L_m}, \\ \frac{dv_C}{dt} &= \frac{Ni_{Lm}}{C} - \frac{v_C}{RC}. \end{aligned} \quad (3)$$

The average form of  $t_{on}$  and  $t_{off}$  is as follows:

$$\begin{aligned} \frac{di_{Lm}}{dt} &= -\frac{Ni_{Lm}(1-d)}{L_m} + \frac{dV_i}{L_m}, \\ \frac{dv_C}{dt} &= -\frac{Ni_{Lm}(1-d)}{C} - \frac{v_C}{RC}. \end{aligned} \quad (4)$$

### 3. State-Space Model of Non-Linear CCM Flyback Converter

To apply feedback linearisation, we need to know the state-space description of the system. We have already presented a detailed representation of these for switch-mode converters.

Accordingly, the state-space averaged model of the CCM flyback converter in the matrix form is as follows (Howimanporn and Bunlaksananusorn, 2003; Iqbal and Abbas, 2014; Sucu, 2011):

$$\frac{d}{dt} \begin{bmatrix} i_{L_m} \\ v_c \end{bmatrix} = \begin{bmatrix} 0 & -\frac{N(1-d)}{L_m} \\ \frac{N(1-d)}{C} & -\frac{1}{RC} \end{bmatrix} \begin{bmatrix} i_{L_m} \\ v_c \end{bmatrix} + \begin{bmatrix} d \\ 0 \end{bmatrix} \frac{V_i}{L_m}, \quad (5)$$

where  $i_{L_m}$  and  $v_c$  represent the current of the magnetising inductor and voltage of the output capacitor (output voltage), respectively;  $V_i$  is the input DC voltage; R, L, C and N symbolise the output load, inductance, capacitance and turn ratio, respectively; and  $d$  denotes the duty cycle of the converter. Figure 1 shows the topology of the flyback converter.

A single-input single-output (SISO) non-linear system can be written as follows (Csizmadia et al., 2022; Csizmadia and Kuczmann, 2022; Zheng and Shuai, 2012):

$$\begin{cases} \dot{x} = f(x) + g(x)u, \\ y = h(x), \end{cases} \quad (6)$$

where

$$f(x) = \begin{bmatrix} -\frac{N}{L_m}v_c \\ \frac{N}{C}i_{L_m} - \frac{1}{RC}v_c \end{bmatrix} \quad (7)$$

$$g(x) = \begin{bmatrix} \frac{N}{L_m}v_c + \frac{V_i}{L_m} \\ -\frac{N}{C}i_{L_m} \end{bmatrix} \quad (8)$$

## 4. Controller Design Applying Exact Feedback Linearisation with Integrator

Several previous articles have reviewed the method in detail, so only the results are used here. Let the controlled quantity be the output (capacitor) voltage, that is:

$$y = v_c. \quad (9)$$

Differentiating  $y$  with respect to time, we get the following:

$$\frac{dy}{dt} = \frac{N(1-d)i_{L_m}}{C} - \frac{v_c}{RC}. \quad (10)$$

It is visible that the relative degree of the system is  $r < n$ . In order for  $g(x) = 0$ , we choose a new state variable; therefore:

$$\frac{\partial h}{\partial x} [g(x)] = 0. \quad (11)$$

The solution of (Frobenius type) Eq. (15) is as follows (Csizmadia et al., 2022; Csizmadia and Kuczmann, 2022; Zheng and Shuai, 2012):

$$h(x) = \frac{Ni_L^2}{C} + \frac{2v_iv_c + Nv_c^2}{L_m}. \quad (12)$$

Accordingly, the transformation matrix is given by the following expression:

$$[\mathbf{T}(x)] = z = \begin{bmatrix} h(x) \\ L_f h(x) \end{bmatrix}. \quad (13)$$

The control input of the flyback converter is achieved as follows:

$$u = \frac{-L_f h(x) + v}{L_g L_f^{(r-1)} h(x)}. \quad (14)$$

The Lie derivatives of Eqs. (13) and (14) are shown in the Appendix. The system diagram with the measured parameters is shown in Figure 3.

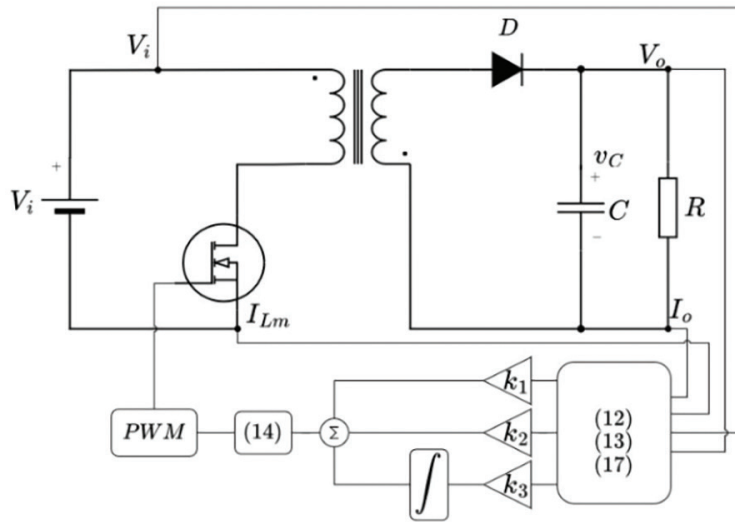


**Fig. 3.** Block diagram of feedback linearised scheme. R, L and C symbolise the output load, inductance and capacitance, respectively, of the converter.  $L_m$ , magnetising inductance; WM, pulse width modulator.

## 5. Feedback Design

In the previous section, the non-linear system is transformed into a linear system; so,

$$\begin{cases} \dot{z}_1 & 0[z_1] + 1[v] \\ \dot{z}_2 & [h(x)] \\ y & [z_1] \end{cases}. \quad (15)$$

Accordingly, the internal controller must be designed for this linearised system.

### 5.1. Reference value calculation

The system is controllable in case the output function is equal to that in Eq. (12). Accordingly, the second state variable  $i_{L_m}$  needs to be expressed by other parameters. To find the steady-state variable, ( $d$  and  $i_{L_m}$ ) need to nullify the time derivatives (Cervone and Brando, 2020). So,

$$\begin{aligned} d &= \frac{Nv_{ref}}{v_i + Nv_{ref}} \\ i_{L_m} &= \frac{dV_i}{R(1-d)^2 N^2} \end{aligned}. \quad (16)$$

As a result, the equivalent reference function is selected as follows:

$$h_{ref} = \frac{\left( \frac{\frac{v_{ref}}{R}}{1 - \frac{v_c - V_i}{V_i}} \right)^2}{C} + \frac{v_{ref}^2}{L_m}. \quad (17)$$

## 5.2. Linear controller design

The internal linear controller should be designed for Eq. (15) and can be realised by some classical control methods, such as the proportional–integral–derivative (PID) controller, linear quadratic regulator (LQR) or state feedback. In our case, the control was realised by pole placement (Ackermann method). Accordingly, the poles were determined as follows (Keviczky et al., 2011):

$$p = [-1 / 0.0001; -1 / 0.001; -1 / 0.0005]. \quad (18)$$

So, the feedback gain ( $k$ ) matrix is chosen as follows:

$$k^T = [32,000,000, 13,000, 2 \cdot 10^{11}]. \quad (19)$$

## 6. Simulation Results and Conclusion

The flyback converter was introduced and analysed by Kirchhoff's laws in the second chapter and described in a state-space form in the third chapter. To make our work more comparable, we chose a non-linear controller, namely an SMC, as a reference work. At the same time, we also designed an optimal controller, that is, a LQ controller, based on a previously published paper, so that we can directly compare the results (Csizmadia and Kuczmann, 2020). Accordingly, the parameters of the investigated flyback converter are summarised in Table 1. The parameters of the LQ controller are given in the Table 2, and the block scheme of the LQ controller-based system is shown in Figure 4.

To investigate the dynamic, steady-state and robust behaviour, the following tests were examined: reference voltage variation, load variation, input voltage change and nominal start-up. Accordingly, Figures 5 and 6 show the

Symbol	Value
$R_{nom}$	10 $\Omega$
$L_m$	250 $\mu$ H
$C$	200 $\mu$ F
$N$	0.5
$V_i$	12 V
$V_o$	24 V
$I_o$	2.4 A
$f_{sw}$	100 kHz

**Table 1.** Flyback converter parameters.

Symbol	Value
$k_1$	0.096
$k_2$	0.088
$k_i$	141.4

LQ, linear quadratic.

**Table 2.** LQ controller parameters.

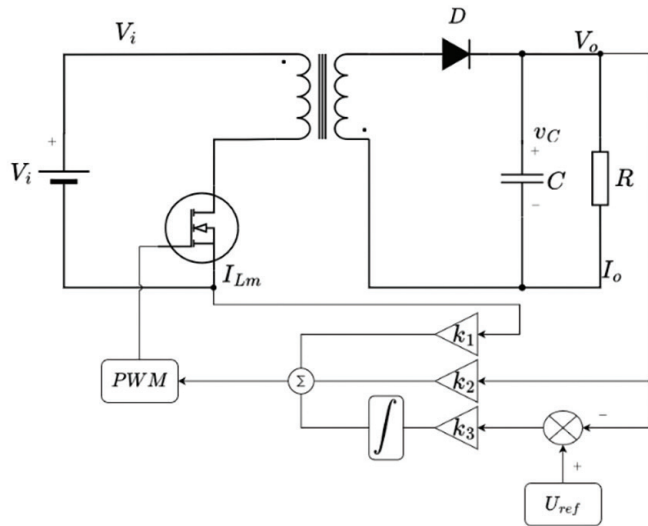


**Fig. 4.** Block diagram of LQ control of flyback converter. R, L and C symbolise the output load, inductance and capacitance, respectively, of the converter.  $L_m$ , magnetising inductance; LQ, linear quadratic; PWM, pulse width modulator.

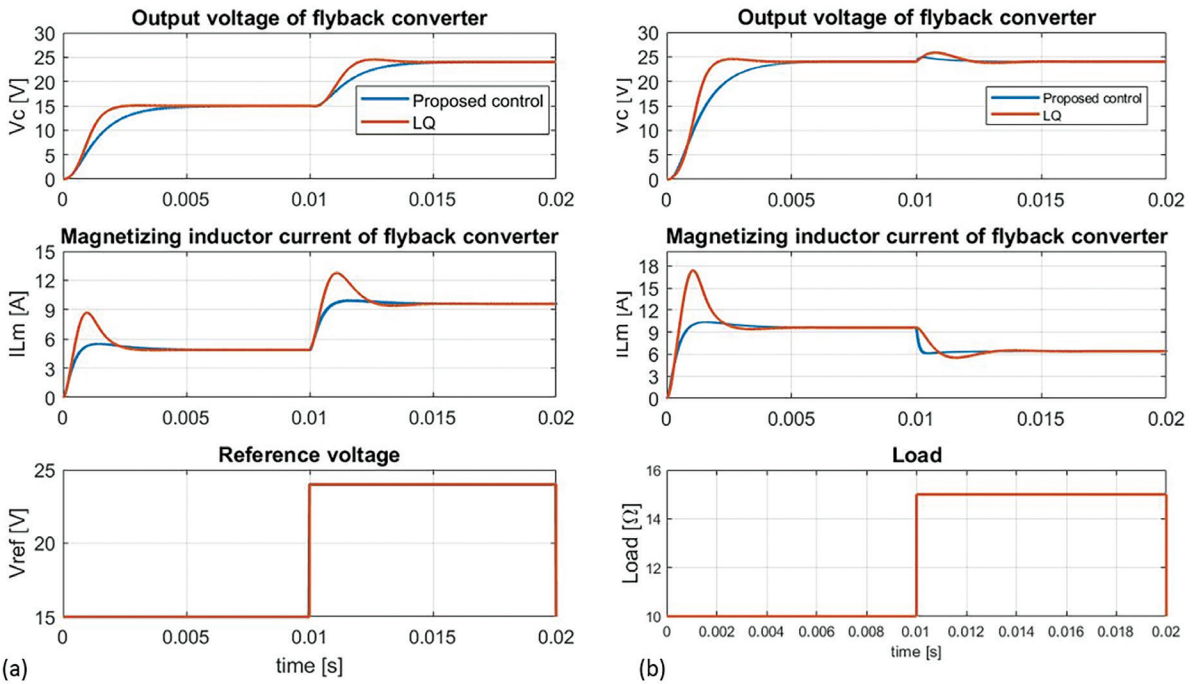


**Fig. 5.** (a) Response on reference voltage change from 10 V to 25 V, and (b) output load variation from 10 Ω to 15 Ω. LQ, linear quadratic.

response of the main system parameters, that is, capacitor voltage and transformer magnetising current, to the dynamic and steady-state tests for the linear quadratic and the proposed novel feedback linearisation controller, respectively. All simulations were run for 20 ms, and changes were made at half of the time interval, that is, at 10 ms (except for the steady-state simulation). Figure 5a shows the reference voltage variation test. The reference voltage changed from 15 V to 24 V. Figure 5a shows that the capacitance voltage is very accurate for both regulators; at the same time, the presented regulator follows the variation of the reference voltage without overshoot. The clear difference is in the magnetising current of the transformer: the proposed regulator has no inrush current, unlike the

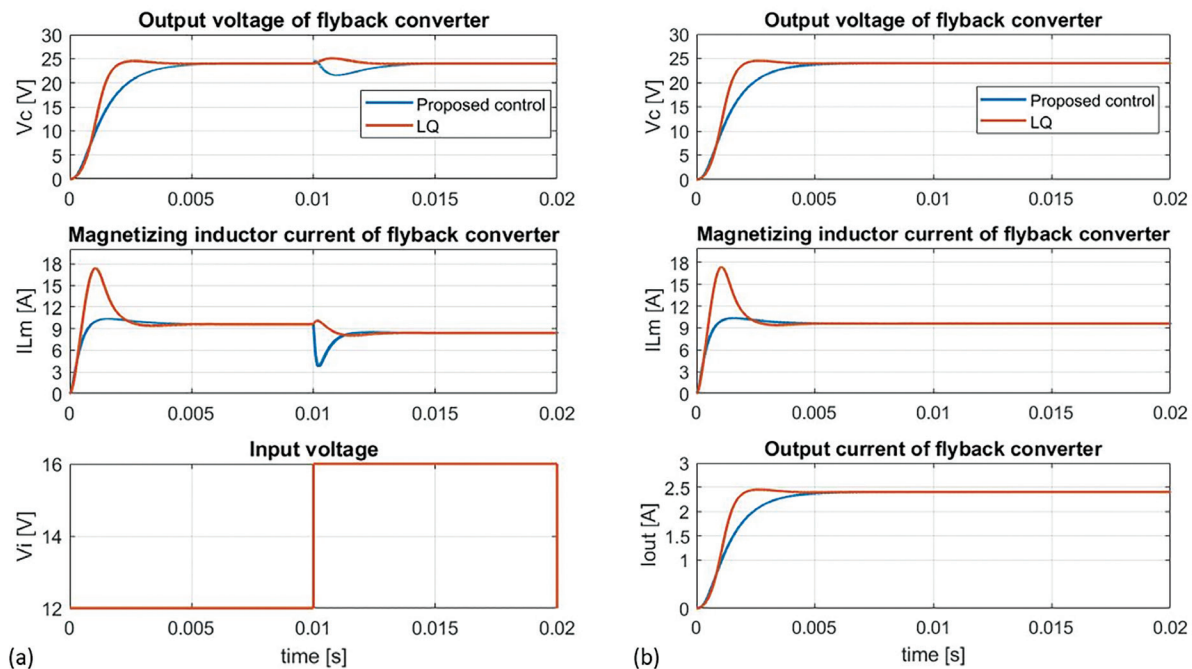


**Fig. 6.** Response on input voltage variation from 12 V to 16 V, and start-up/steady-state simulation results.  $L_m$ , magnetising inductance; LQ, linear quadratic.

LQ regulator. Figure 5b shows the output load variation test. The load resistance value has been changed from the designed  $10\ \Omega$  to  $15\ \Omega$ . The proposed controller has a smaller transient error in capacitor voltage, namely 1 V (4%). However, the transient interval is smaller for the proposed controller. A significant inrush current of the magnetic inductor is observed only during the test start-up for the LQ controller. For the input voltage variation (Figure 6a), the two regulators show almost identical transient responses. The magnetising current of the transformer shows a similar shape as in the previous test. In the start-up test (Figure 6b), the following conclusions can be drawn: for the presented regulator, there is no overshoot in either the capacitance voltage or the transformer magnetising current.

By comparing the simulation results with the results of the reference paper, it can be concluded that in the case of the proposed controller, there is no overshoot in the controlled quantity (capacitance–voltage) in any of the tests.

## 7. Conclusions

In this paper, a novel feedback linearisation of the CCM flyback converter is presented. The control methods reported in the literature show independently good results, but almost all of them have some problems, such as inrush current, steady-state error, non-robust behaviour or high transient overshoot. This paper proposed the application of an error integrator in the feedback linearisation control loop, and the simulation results of this method are compared with those from a non-linear and optimal control algorithm. As shown from the simulation results, this new form of feedback linearisation exhibits very good transient and steady-state behaviour. Moreover, the controller design can be transformed into a framework, which makes the design faster and more robust. Future plans include laboratory tests and sensorless implementation for good practical applicability.

## References

- H. A. Bouziane, R. B. Bouiadjra and M. B. Debbat, "Design of robust LQR control for DC-DC multilevel boost converter," 2015 4th International Conference on Electrical Engineering (ICEE), Boumerdes, Algeria, 2015, pp. 1-5, doi: 10.1109/INTEE.2015.7416728.
- Cervone, A. and Brando, G. (2020). Input-State feedback linearization of a boost DC/DC converter, pp. 139–153.

- Csizmadia, M. and Kuczmann, M. (2020). Design of LQR Controller for GaN Based Buck Converter. *Pollack Periodica* 15(2), pp. 37–48. doi: 10.1556/606.2020.15.2.4.
- Csizmadia, M. and Kuczmann, M. (2022). Extended Feedback Linearization Control of Non-ideal DCDC Buck Converter in CCM. *Power Electronics and Drives*, 7(42).
- Csizmadia, M., Kuczmann, M. and Orosz, T. (2022). A Novel Control Scheme Based on Exact Feedback Linearization Achieving Robust Constant Voltage for Boost Converter. *Electronics*, 12(1), p. 57. doi: 10.3390/electronics12010057.
- Howimanporn, S. and Bunlaksananusorn, C. (2003). Performance comparison of continuous conduction mode (CCM) and discontinuous conduction mode (DCM) flyback converters. In: *The Fifth International Conference on Power Electronics and Drive Systems, 2003. PEDS 2003*, Vol. 2, pp. 1434–1438. doi: 10.1109/PEDS.2003.1283194.
- Iqbal, H. K. and Abbas, G. (2014). Design and analysis of SMC for second order DC-DC flyback converter. In: *17th IEEE International Multi Topic Conference 2014*, pp. 533–538. doi: 10.1109/INMIC.2014.7097398.
- Keviczky, L., Bars, R., Hetthéssy, J. and Bányász, C. (2011). *Control Engineering*. Hungary: Széchenyi István University.
- Khairy, S., Abozied, H., El-Zohri, E. H. and El Sayed, R. A. (2015). Self-Oscillating Flyback Converter for Mobile Batteries Charging Applications.
- Mandal, S. and Mishra, D. (2018). Robust control of buck converter using H-infinity control algorithm. In: *2018 IEEE Applied Signal Processing Conference (ASPCON)*, pp. 163–167. doi: 10.1109/ASPCON.2018.8748623.
- Mohammed, A. A. and Nafie, S. M. (2015). Flyback converter design for low power application. In: *2015 International Conference on Computing, Control, Networking, Electronics and Embedded Systems Engineering (ICCNEEE)*, pp. 447–450. doi: 10.1109/ICCNEEE.2015.7381410.
- Mohanty, P. R., Panda, A. K. and Das, D. (2015). An active PFC boost converter topology for power factor correction. In: *2015 Annual IEEE India Conference (INDICON)*, New Delhi, pp. 1–5. doi: 10.1109/INDICON.2015.7443118.
- Pesce, C., Riedemann, J., Peña, R., Degano, M., Pereda, J., Villalobos, R., Maury, C., Young, H. and Andrade, I. (2021). A Modified Multi-Winding DC–DC Flyback Converter for Photovoltaic Applications. *Applied Sciences*, 11, p. 11999. doi: 10.3390/app112411999.
- Prasad, G. and Kumar, A. (2018). A comparison between sliding mode control and feedback linearization. In: *2018 5th IEEE Uttar Pradesh Section International Conference on Electrical, Electronics and Computer Engineering (UPCON)*, pp. 1–5. doi: 10.1109/UPCON.2018.8597038.
- Paul, M. M. R. and Bhuvanesh, A. (2015). Design and Implementation of Battery Charger Using Flyback Converter for Constant Current and Voltage Control. *International Journal for Research in Applied Science and Engineering Technology*, 3, pp. 153–159.
- Ramos-Paja, C. A., Bastidas-Rodriguez, J. D. and Saavedra-Montes, A. J. (2021). Design and Control of a Battery Charger/Discharger Based on the Flyback Topology. *Applied Sciences*, 11, p. 10506. doi: 10.3390/app112210506.
- Sucu, M. (2011). *Parametric average value modeling of flyback converters in CCM and DCM including parasitics and snubbers (T)*. University of British Columbia. Available at: <https://open.library.ubc.ca/collections/ubctheses/24/items/1.0072322>. (last check 2023.01.13)
- Szeli, Z., Horváth, E. and Szakállas, G. (2013). Versenyautó telemetriás rendszerének fejlesztése, különös tekintettel a rendszer villamosmérnöki és informatikai vonatkozásaira, A jövő járműve, 2013/01/02, pp. 42–45.
- Tseng, S.-Y. and Fan, J.-H. (2021). Buck-Boost/Flyback Hybrid Converter for Solar Power System Applications. *Electronics*, 10, p. 414. doi: 10.3390/electronics10040414.
- Yin, Q., Gan, J., Chen, T., Shi, W., Liu, X. and Chang, Z. (2020). Research on the flyback switch power supply based on the primary feedback and the valley control. In: *2020 IEEE 9th Joint International Information Technology and Artificial Intelligence Conference (ITAIC)*, pp. 1312–1315. doi: 10.1109/ITAIC49862.2020.9338942.
- Zheng, H. and Shuai, D. (2012). Nonlinear control of Boost converter by state feedback exact linearization. In: *2012 24th Chinese Control and Decision Conference (CCDC)*, pp. 3502–3506.

## Appendix

The Lie derivatives of the flyback converter are as follows:

$$L_f h(x) = \frac{(2V_i + 2Nv_c) \left( \frac{v_c}{RC} - \frac{Ni_{Lm}}{C} \right)}{L_m} - \frac{2N^2 i_{Lm} v_c}{CL_m}, \quad (\text{A1})$$

$$L_f^2 h(x) = \left( \frac{v_c}{RC} - \frac{Ni_L}{C} \right) \left( \frac{2N \left( \frac{v_c}{RC} - \frac{Ni_{Lm}}{C} \right)}{L_m} + \frac{2V_i + 2Nv_c}{RCL_m} + \frac{2N^2 i_L}{CL_m} \right) - \frac{Nv_c \left( \frac{N(2V_i + 2Nv_c)}{CL_m} - \frac{2N^2}{CL_m} \right)}{L_m}, \quad (\text{A2})$$

$$L_g L_f h(x) = \frac{\left( \frac{N(2V_i + 2Nv_c)}{CL_m} - \frac{2N^2}{CL_m} \right) (V_i + Nv_c)}{L_m} + \frac{Ni_{Lm} \left( \frac{2N \left( \frac{v_c}{RC} - \frac{Ni_{Lm}}{C} \right)}{L_m} + \frac{2V_i + 2Nv_c}{RCL_m} + \frac{2N^2 i_{Lm}}{CL_m} \right)}{C}. \quad (\text{A3})$$